STM JOURNALS

Journal of
Polymer & Composites

ISSN: 2321-2810 (Online)
ISSN: 2321-8525 (Print)
Volume 13, Special Issue 2, 2025
DOI (Journal): 10.37591/JoPC

https://journals.stmjournals.com/jopc

Research JoPC

Affect of Finite Element Modelling on Static Behavior of Underwater Shell

Jayanth Datta Thota[1,*], Navaneeth Manikonda[2], Venkateswararao Mendol[3], Balakrishna Murthy Vallabhaneni [4]

Abstract

The objective of the present study is to compare and contrast different numerical models based on their mesh quality and material properties in predicting the response of an underwater shell under an external pressure of 1 MPa. Two different mesh qualities with the same element size are developed for solid geometries without and with slicing the solids at geometric discontinuities to enhance the element quality. From the static response of the structure from both the solid models, variation in deformation and stresses is observed due to changes in element quality for the same size. The observed difference of around 2.5% in the results between the converged sliced model and the corresponding non-sliced model highlights the impact of mesh quality and modeling approach on the accuracy of the simulation. Extending the analysis by replacing the aluminum shell casing with carbon-epoxy composite (CFRP) introduces an additional layer of complexity due to the material properties and behavior of CFRP compared to aluminum. The comparison between the results obtained from the sliced model with CFRP and aluminum shell casings will provide insights into how the change in a material affects the structural response under external pressure. The entire process is executed using ANSYS software.

Keywords: Resin, epoxy, underwater capsule, element quality, mechanical properties, solid-shell model, FEA

INTRODUCTION

Underwater capsules are chambers designed to withstand the immense pressure of deep-sea environments. These capsules serve as vital conduits for scientific research, marine exploration, and immersive underwater experiences, research, or observation beneath the surface of the water. This paper concentrates on differentiating various numerical models in terms of mesh quality and geometry to predict the responses of an underwater capsule. According to More and Bindhu have presented a study of the effects of mesh size on the accuracy of numerical analysis results, conducting static and buckling analyses using Femap and NX-Nastran [1]. Park and Shontz proposed a mesh quality metric alternation scheme that enhances efficiency by alternating between original and more efficient metrics during iterations, accelerating convergence compared to conventional methods [2]. Amit and Azim studied the critical role of Computer-Aided Engineering in product design, particularly in Finite Element Analysis, aiming to identify the most effective approach for obtaining accurate results while minimizing computational time [3]. Aman Dutt presented a paper on the influence of mesh size on result accuracy in FEA using Creo 2.0 software, providing insights from a cantilever model under

***Author for Correspondence**
Jayanth Datta Thota

[1,2,3] UG Student, Department of Mechanical Engineering, V. R. Siddhartha Engineering College, Siddhartha Academy of Higher Education (Deemed to be University), Vijayawada, Andhra Pradesh, India
[4]Professor, Department of Mechanical Engineering, V. R. Siddhartha Engineering College, Siddhartha Academy of Higher Education (Deemed to be University), Vijayawada, Andhra Pradesh, India

Received Date: May 01, 2024
Accepted Date: October 21, 2024
Published Date: January 22, 2025

Citation: Jayanth Datta Thota, Navaneeth Manikonda, Venkateswararao Mendol, Balakrishna Murthy Vallabhaneni. Affect of Finite Element Modelling on Static Behavior of Underwater Shell. Journal of Polymer & Composites. 2025; 13(Special Issue 2): S154–S163p.

uniform load to improve FEA simulation accuracy [4]. Ping employed SolidWorks and ANSYS Workbench to analyze the deformation and stress distribution in a cylinder head during disassembly and assembly [5]. Irfan Sadaq's research assessed the burst pressure of composite material pressure vessels using ANSYS simulations across various fiber angles and composite types, validating deformation, stress, and strain outcomes [6]. Raut compared linear and quadratic tetrahedral elements with hexahedral elements in structural analyses, revealing equivalent accuracy and offering insights into choosing element types based on specific simulation needs [7]. Liu examined the significance of element size in finite element models across static analysis, offering guidelines for balancing simulation accuracy and computational simplicity [8]. Freitag and Ollivier proposed methods to enhance mesh quality for efficient solving of complex 3D problems, emphasizing the importance of element shape [9]. Semih and Selim modeled an AISI 310 stainless steel cylinder using ANSYS Workbench 12.0, analyzing stress and deformation under a 1000 N y-axis force, revealing stress concentration at the cylinder's ends using FEM [10].

PROBLEM MODELLING

Numerical geometries of underwater capsules were created in two models of solid (i.e.) without slicing and with slicing at geometrical discontinuities. A finite element mesh was generated, and convergence was checked. The results from the static analysis were compared for both the models. The results of the converged sliced model are taken into consideration due to the high element quality. Shell parts are made up of carbon-epoxy composite (CFRP) and the results were compared with the solid model.

GEOMETRY

Geometry is modeled in Ansys workbench geometry. Figure 1 shows geometry.

Dimensions of the Underwater Capsule: The total length of the capsule is 1125 mm.

The outer Diameter is 250 mm, the Inner Diameter is 240 mm, the thickness is 5 mm, the width of the flange is 6.5 mm, the width of the cap is 8 mm, the length of the cylinders is 489.5 mm, the End cap width is 7 mm.

Parts are a hemispherical dome, 2 cylinders, 4 flanges, 2 caps, 1 end cap. The first 2 flanges join the hemispherical dome and 1st cylinder; the 1st cap holds the 2 flanges. The same is done for connecting the 2 cylinders. The end cap is made to close the other end.

MATERIALS

Material used for the solid models is aluminum. Table 1 shows the mechanical properties of aluminum.

Table 1. Properties of Aluminum.

Property	Value	Units
Density [ρ]	2770	kg m^-3
Young's Modulus [E]	71000	MPa
Poisson's Ratio [ν]	0.33	-
Bulk Modulus [K]	69608	MPa
Shear Modulus [G]	26692	MPa

Material used for the shell model is carbon-epoxy composite (CFRP). Table 2 shows the properties of CFRP.

Journal of Polymer & Composites
Volume 13, Special Issue 2
ISSN: 2321-2810 (Online), ISSN: 2321-8525 (Print)

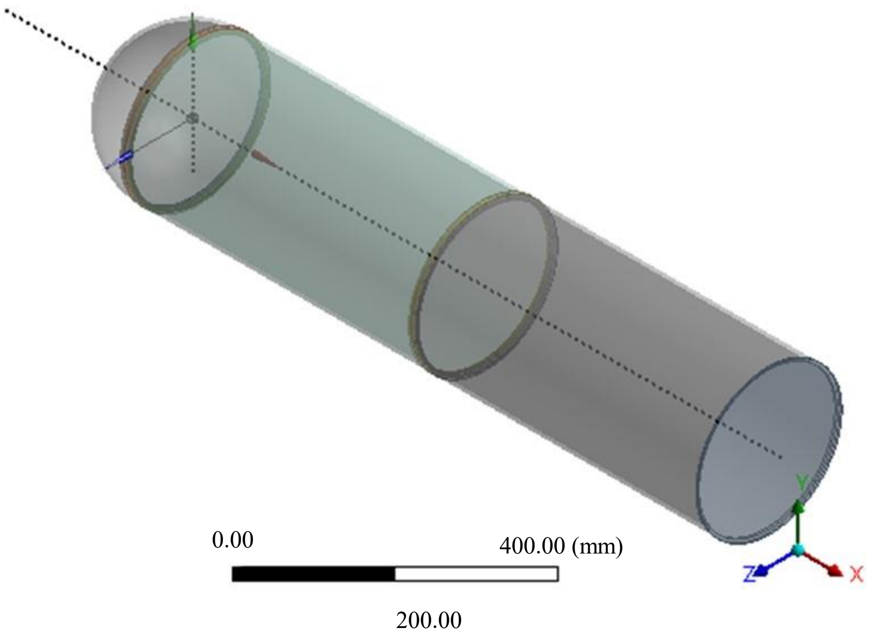

Figure 1. Underwater capsule.

Table 2. Properties of carbon-epoxy composite.

Property	Value	Units
Density [ρ]	1518	[kg m^-3]
Young's Modulus X direction [Ex]	1.23E+05	MPa
Young's Modulus Y direction [Ey]	7780	MPa
Young's Modulus Z direction [Ez]	7780	MPa
Poisson's Ratio XY [ν_{xy}]	0.27	-
Poisson's Ratio YZ [ν_{xy}]	0.42	-
Poisson's Ratio XZ [ν_{xy}]	0.27	-
Shear Modulus XY [Gxy]	5000	MPa
Shear Modulus YZ [Gyz]	3080	MPa
Shear Modulus XZ [Gxz]	5000	MPa

Table 3 shows fiber angle data at each layer.

Table 3. Fiber Angle Data.

Layer	Fiber angle
L1	90°
L2	90°
L3	45°
L4	-45°
L5	90°
L6	90°
L7	-45°
L8	45°
L9	90°
L10	90°

FINITE ELEMENT MESH

The meshing for the model is done with quadratic element order as it gives more accurate results. For the finite element mesh refer to Figure 2. Element size = 6mm.

Figure 2. Finite element mesh.

CONVERGENCE

The models were meshed with Quadratic element order with different element sizes. The model global element size starts at 15mm, 10 mm, 8 mm, 7 mm, 6 mm, 5 mm, and finally 4mm. The same element sizes are taken for the flanges and caps. Total deformation results were taken into consideration for convergence.

Table 4. Without Slicing Model.

Global element size [mm]	Element size for flanges and caps [mm]	Ur [mm]	%variation [%]
15	15	6.90E-02	
10	10	6.94E-02	-0.48539
9	9	7.00E-02	-0.88968
8	8	6.89E-02	1.46638
7	7	6.87E-02	0.293
6	6	6.87E-02	0.08147
5	5	6.84E-02	0.41349
4	4	6.80E-02	0.61404

Table 4 shows the values of total deformations corresponding to the change in element size of the model without slicing. The graphical representation of the variations is shown in Figure 3.

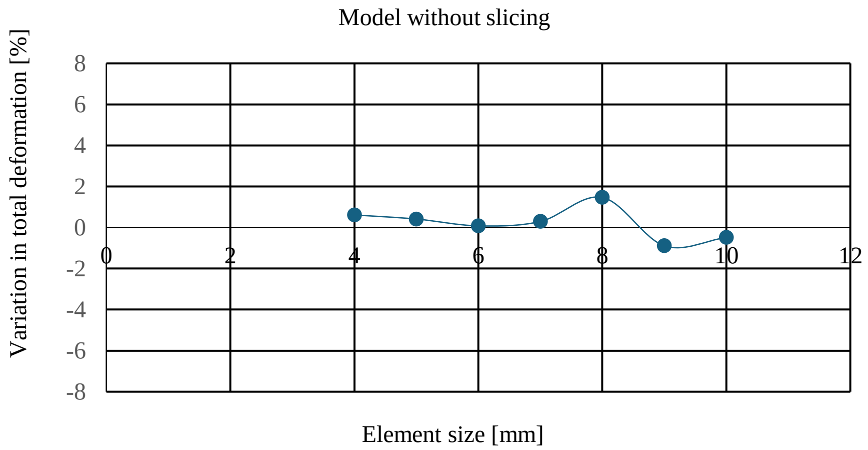

Figure 3. Element size vs variation in total deformation graph (Without Slicing).

From Figure 3 for the model without slicing it is observed that as the element size reaches 6 mm, the variations in deformations observed begin to show minimal with further change in element size. This indicates that refinement of the mesh further does not significantly affect the results.

Table 5 shows the values of total deformations corresponding to the change in element size of the model with slicing. The graphical representation of the variations is shown in Figure 4.

From Figure 4 for the sliced model, it is observed that as the element size reaches 6 mm, the deformations observed begin to show minimal with further change in element size. This indicates that refinement of the mesh further does not significantly affect the results.

After observation of the convergence of results, the 6mm element size was fixed for the convergence size for the analysis. The results of the converged sliced model are taken into consideration due to the high element quality.

RESULTS AND DISCUSSION

The results taken from both models with the converged element size are compared.

Radial Deformation [Ur]

Table 6 gives the variation in radial deformation at element size 6mm. The variation between the values of the model without slicing and with slicing is 0.328819615%.

Table 5. With Slicing Model.

Global element size [mm]	Element size for flanges and caps [mm]	Ur [mm]	%variation [%]
15	15	6.85E-02	
10	10	6.99E-02	-2.06693
9	9	6.94E-02	0.62255
8	8	6.83E-02	1.59853
7	7	6.83E-02	0.00585
6	6	6.83E-02	-0.00585
5	5	6.81E-02	0.27368
4	4	6.74E-02	1.11825

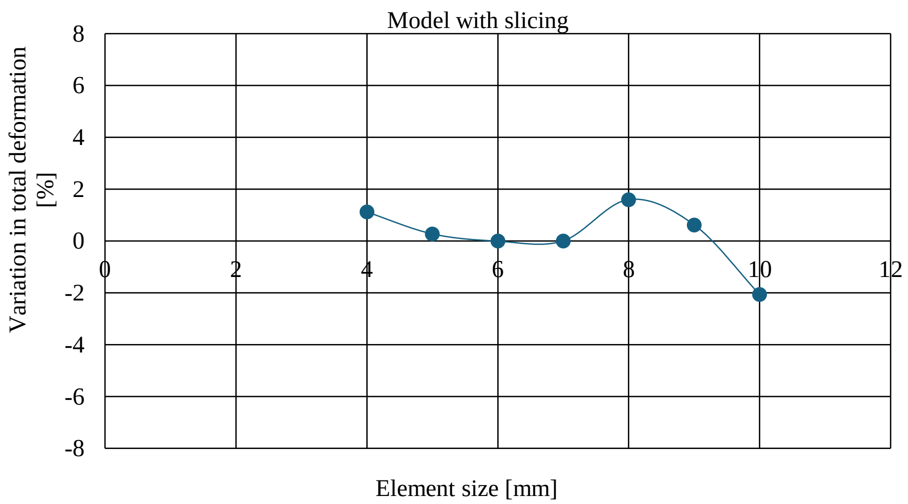

Figure 4. Element size vs variation in total deformation graph (With slicing).

Table 6. Radial Deformation.

Global element size [mm]	Element size for flanges and caps [mm]	Ur-without slicing [mm]	Ur-with slicing [mm]	%variation [%]
6	6	3.86E-02	3.85E-02	0.328819615

The contours are shown below in Figure 5 & Figure 6.

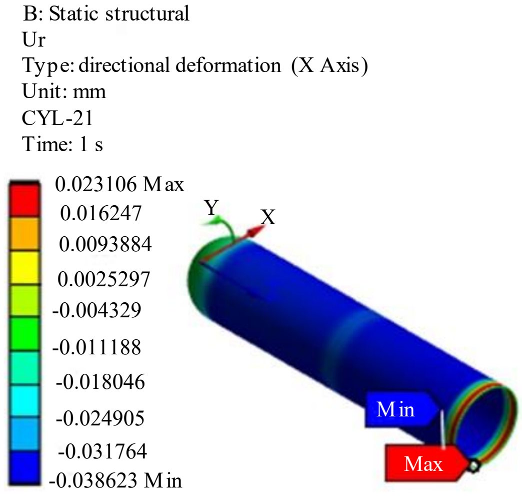

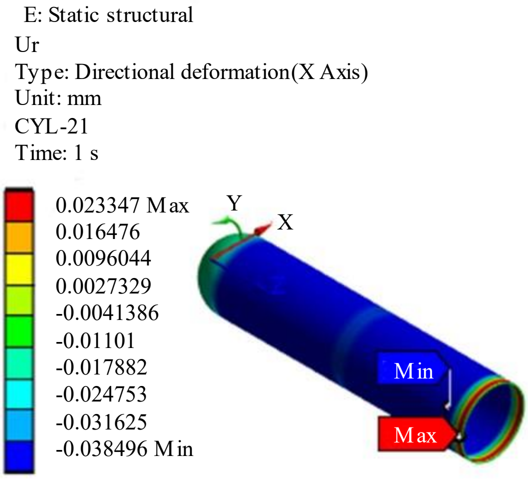

Figure 5. The contour of the model without slicing. **Figure 6.** The contour of the model with slicing

Figure 5 and Figure 6 show the maximum and minimum values of radial deformation. Ur$_{max}$ and Ur$_{min}$ occur at the 2nd cylinder in both models.

Axial Deformation [Ua]

Table 7 gives the variation in axial deformation at element size 6mm. The variation between the values of the model without slicing and with slicing is 0.481536%.

Table 7. Axial Deformation.

Global element size [mm]	Element size for flanges and caps [mm]	Ua-Without slicing [mm]	Ua-With slicing [mm]	%variation [%]
6	6	6.87E-02	6.83E-02	0.481536

The contours are shown below in Figure 7 & Figure 8.

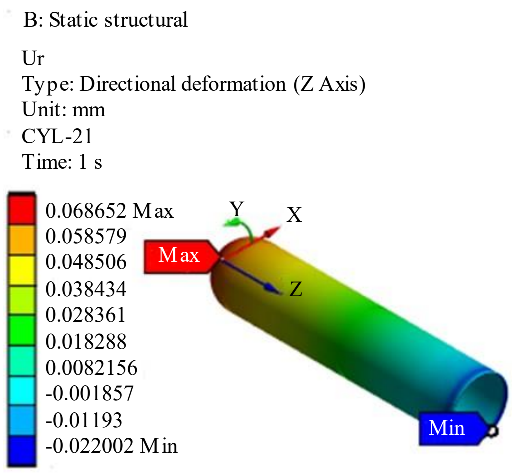

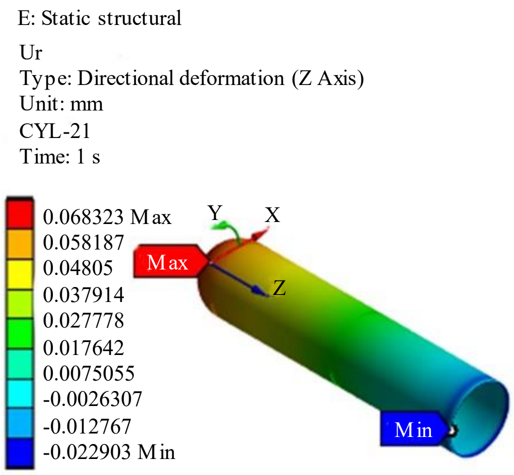

Figure 7. The contour of the model without slicing **Figure 8.** The contour of the model with slicing

Journal of Polymer & Composites
Volume 13, Special Issue 2
ISSN: 2321-2810 (Online), ISSN: 2321-8525 (Print)

Figure 7 and Figure 8 show the maximum and minimum values of axial deformation. Ua_{max} and Ua_{min} occur at the hemispherical dome and 2nd cylinder respectively in both the models.

Total Deformation [Ut]

Table 8 gives the variation in total deformation at element size 6mm. The variation between the values of the model without slicing and with slicing is 0.51686%.

Figure 9 and Figure 10 show the maximum and minimum values of total deformation. Ut_{max} And Ut_{min} occur at the hemispherical dome and 2nd cylinder respectively in both the models.

Von-Mises [Equivalent Stress]

Table 9 gives the variation in Von Mises at element size 6mm. The variation between the values of the model without slicing and with slicing is 2.557521313%.

Table 9. Von-mises.

Global element size [mm]	Element size for flanges and caps [mm]	Max stress without slicing [mm]	Max stress with slicing [mm]	%variation [%]
6	6	109.09	106.3	2.557521313

Table 8. Total Deformation.

Global Element size [mm]	Element size for flanges and caps [mm]	Ut-without slicing [mm]	Ut-with slicing [mm]	%variation [%]
6	6	6.87E-02	6.83E-02	0.51686

The contours are shown below in Figure 9 & Figure 10.

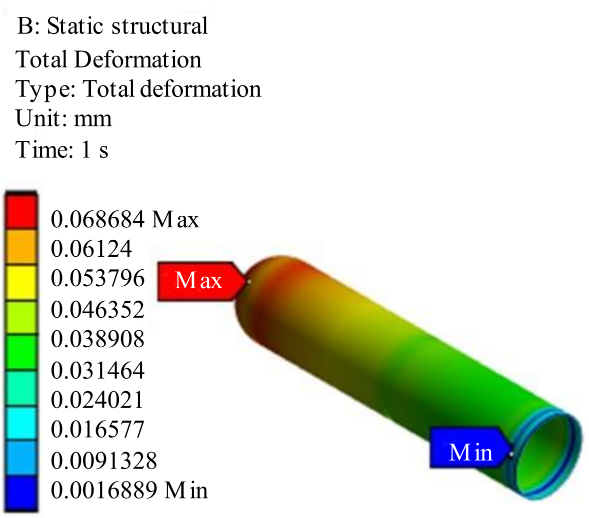

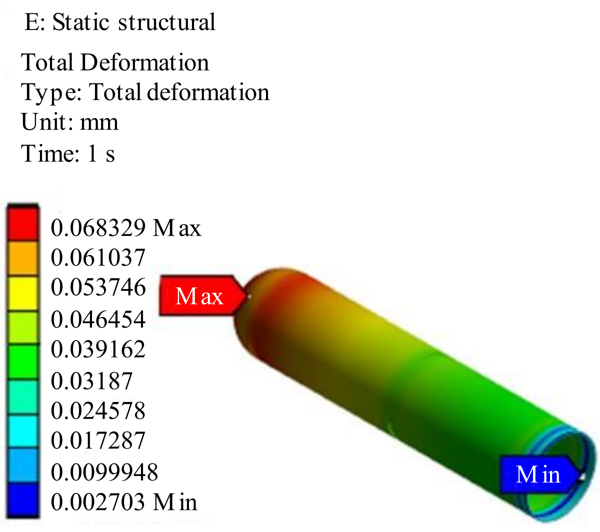

Figure 9. The contour of the model without slicing **Figure 10.** The contour of the model with slicing

The contours are shown below in Figure 11 & Figure 12.

Figure 11 and Figure 12 show the maximum and minimum values of stresses. $stress_{max}$ and $stress_{min}$ occur at 2nd in both the models.

Refer to Table 10 for Mesh Quality, nodes, and elements in converged models.

Results of Composite Shell Model

Table 11 gives the values of Deformations in the composite model at the element size of 6mm.

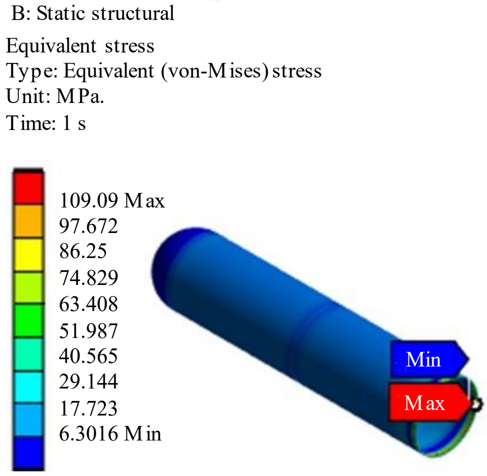

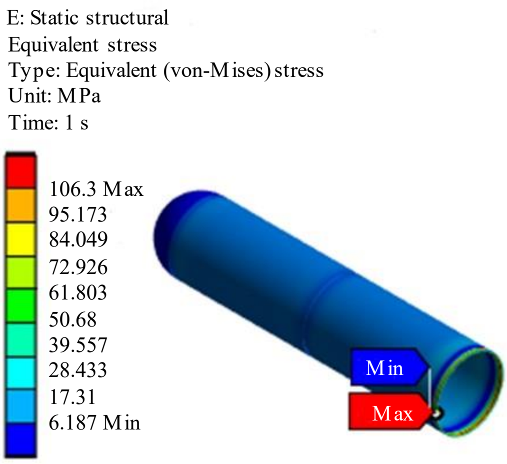

Figure 11. The contour of the model without slicing **Figure 12.** The Contour of the model with slicing

Table 10. Mesh Quality, nodes, and elements in converged models.

	Model without slicing	**Model with slicing**	**%variation**
Mesh Quality	0.76338	0.82499	7.46796931
Number of elements	54535	44554	18.3020079
Number of nodes	220925	230959	4.34449404

Table 11. Deformations.

Mesh quality	**Element size [mm]**	**Ur [mm]**	**Ua [mm]**	**Total deformation [mm]**
0.76064	6	4.43E-02	0.71013	0.71017

Figure 13 shows the contours of radial deformation of the composite model. The contour shows the maximum and minimum values. Ur_{max} and Ur_{min} occur at the hemispherical dome and 1st cylinder respectively.

Figure 14 shows the contours of axial deformation of the composite model. The contour shows the maximum and minimum values Ua_{max} and Ua_{min} occur at the hemispherical dome and 2nd cylinder respectively.

Figure 15 shows the contours of total deformation of the composite model. The contour shows the maximum and minimum values. Ut_{max} And Ut_{min} occur at the hemispherical dome and 2nd cylinder respectively.

Stress in Fiber Layers

Table 12 shows the normal stresses in X & Y directions and shear stress in each layer of fiber starting from the top layer L1 to the bottom layer L10 of the composite shell.

Table 12. Stresses in fiber layers.

Layer	**Sx [MPa]**	**Sy [MPa]**	**Sxy [MPa]**
L1	-44.77	33.441	-4.837
L2	-41.517	27.802	4.2389
L3	163.68	15.099	-14.651
L4	148.07	9.9795	11.054
L5	-41.048	-11.777	2.3061
L6	-41.074	-7.9825	1.6497
L7	-46.702	-3.6913	-3.8224
L8	-71.981	-9.0389	7.4818
L9	-41.165	-17.663	-3.1436
L10	-41.198	-23.336	13.096

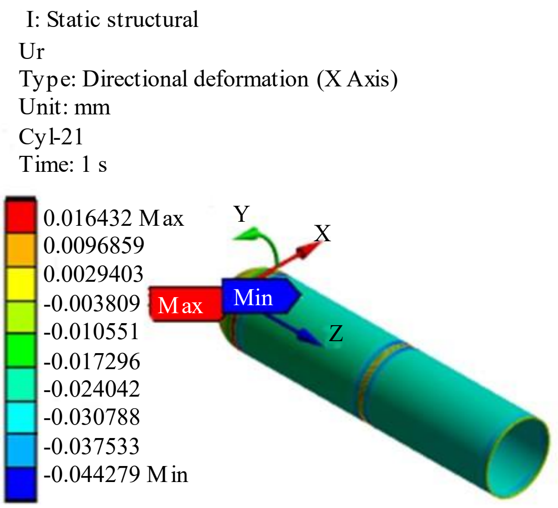

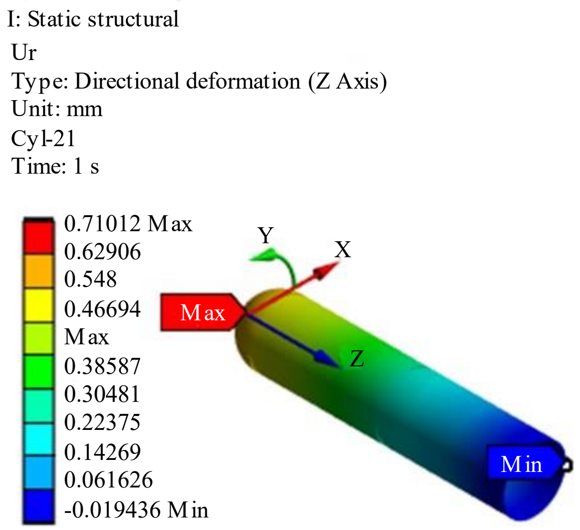

Figure 13. The contour of the model without slicing **Figure 14.** The Contour of the model with slicing

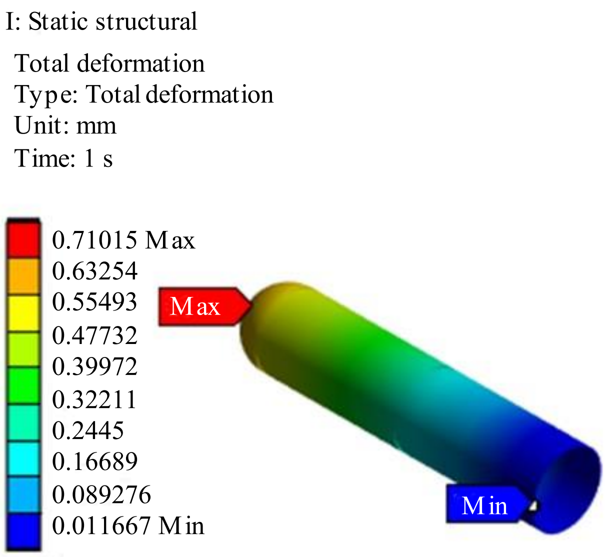

Figure 15. Contour of Total deformation.

CONCLUSION

From the present study on the underwater capsule on responses of static loading. The following conclusions are drawn from the study, which observed that as the element size reaches 6 mm, the deformations observed begin to show minimal variation with further change in element size. Convergence study is made to achieve reasonably acceptable results with minimum computational time. The sliced model yields slightly more mesh quality than the model without slicing because of the geometrical discontinuities. Not much significant variation is observed between the models. The variation in results observed is around 2.5% or less in the results. The composite model with the same thickness is more sensitive as it yields more deformation than the metal model.

REFERENCES

1. More S, Bindhu S. Effect of Mesh Size on Finite Element Analysis of Plate Structure. *International Journal of Engineering Science and Innovation Technology (IJESIT)*. 2015;4(3):23-30.
2. Park J, Shontz SM. An Alternating Mesh Quality Metric Scheme for Efficient Mesh Quality Improvement. *International Conference on Computational Science (ICCS)*; 2011 Jun 1-3; Singapore. Procedia Computer Science. Elsevier; 2011. 4:292-301.

3. Amit N, Azim S . The Mesh Quality Significance in Finite Element Analysis. *IOSR Journal of Mechanical and Civil Engineering (IOSR-JMCE)*. 2020;17(2):44-48.
4. Dutt A. Effect of Mesh Size on Finite Element Analysis of Beam. *Indian Journal of Medical Ethics.* 2015;2:8-10.
5. Ping H. Finite element structural analysis of cylinder head in different disassembly and assembly orders of connection bolts. *Journal of Qinghai Normal University*. 2011.
6. Irfan SS, Vali SK, Sharif SI. Investigation of hybridized composite pressure vessel. In: Khelifa M, ed. *ICMED Proceedings*; 2021 Sep 10-12; Paris, France. E3S Web of Conferences. EDP Sciences; 2021. 309:1-5.
7. Raut P. Impact of Mesh Quality Parameters on Elements Such as Beam, Shell and 3D Solid in Structural Analysis. *International Journal of Engineering Research and Applications (IJERA)*. 2012;2(6):99-103.
8. Liu Y. Choose the Best Element Size to Yield Accurate FEA Results While Reduce Fe Model's Complexity. *British Journal of Engineering and Technology*. 2013;7(1):13-28.
9. Freitag LA, Ollivier-Gooch C. Tetrahedral Mesh Improvement Using Swapping and Smoothing. *International Journal for Numerical Methods in Engineering.* 1998;40(21):3979-3996.
10. Semih T, Selim T. Investigation of Static Structure Effect According to Axial Coordinates by Using Finite Element Method in Ansys Workbench Software of AISI 310 Austenitic Stainless Cylindrical Model Steel. *International Journal of Scientific and Engineering Research.* 2018;2:65-70.

